IEEE Access
Multidisciplinary | Rapid Review | Open Access Journal

Received October 3, 2021, accepted October 28, 2021, date of publication November 2, 2021, date of current version November 9, 2021.

Digital Object Identifier 10.1109/ACCESS.2021.3124948

Fault Detection and Identification Based on Explicit Polynomial Mapping and Combined Statistic in Nonlinear Dynamic Processes

LIANGLIANG SHANG, KEXIN SHI, CHEN MA, AIBING QIU, AND LIANG HUA
School of Electrical Engineering, Nantong University, Nantong, Jiangsu 226019, China

Corresponding author: Liang Hua (hualiang@ntu.edu.cn)

This work was supported in part by the National Nature Science Foundation of China under Grant 61473159, in part by the Natural Science Fund for Colleges and Universities in Jiangsu Province under Grant 17KJB120010, in part by the Six Talent Peaks Project in Jiangsu Province under Grant XYDXX-091, in part by the Natural Science Foundation of the Jiangsu Higher Education Institutions under Grant 19KJA350002, and in part by the Key Program Science and Technology of Nantong under Grant MS22021032 and Grant MS22020030.

ABSTRACT Single traditional multivariate statistical monitoring methods, such as principal component analysis (PCA) and canonical variate analysis (CVA), are less effective in nonlinear dynamic processes. Monitoring approaches based on radial basis kernel function have been intensively applied. However, an infinite dimension nonlinear mapping is redundant and inefficient. To improve the efficiency of traditional methods and consider the nonlinearity and dynamics simultaneously, this paper proposes canonical variate nonlinear principal component analysis (CV-NPCA) based on explicit polynomial mapping and combined statistic for detecting and identifying faults in nonlinear dynamic processes. There are two main contributions of the proposed method. First, explicit second-order polynomial mapping is introduced to combine CVA with PCA to simultaneously decrease the adverse effects of nonlinearity and dynamics. Second, the Q_c statistic combining residual vectors with residual components is proposed, and a two-dimensional (2D) contribution plot and the variable with the largest contribution based on the Q_c statistic are given for fault identification in the simulation study. Compared with the results of PCA, CVA, kernel principal component analysis (KPCA), nonlinear dynamic principal component analysis (NDPCA) and kernel entropy component analysis (KECA), the proposed method not only has relatively higher fault detection rates and identification rates but also has lower false alarm rates in the numerical simulation process and the benchmark Tennessee Eastman process.

INDEX TERMS Canonical variate, combined statistic, explicit polynomial mapping, fault detection, fault identification, principal component analysis, 2D contribution plot.

I. INTRODUCTION

With the increasing requirements for safe operations in complex industrial processes, fault detection and diagnosis have already attracted significant interest in both industrial and academic communities [1]. A large amount of data containing significant information has been stored in databases because sensor technology and distributed control systems are extensively applied. These valuable data provide great convenience for fault detection and diagnosis research based on data-driven methods. Commonly applied multivariate statistical process monitoring (MSPM) methods based on data-driven approaches, such as principal component analysis (PCA) [2], [3], partial least squares (PLS) [4]–[6] and canonical variate analysis (CVA) [7]–[9], have been intensively investigated for fault detection and diagnosis in complex industrial processes [1]. PCA is one of the most extensively adopted methods because its basic principle is relatively simple [10]. The original data space is decomposed into two subspaces: one is the principal component space containing the common cause variability, and the other is the residual component space containing the process noise. CVA obtains the state vector and residual vector spaces by performing singular value decomposition (SVD) on a covariance matrix, which is assembled from the Hankel matrix of the original data [11]. However, nonlinearity, a dynamic characteristic of process data, widely exists in practical complex industries [12]. MSPM methods based on data-driven

The associate editor coordinating the review of this manuscript and approving it for publication was Francesco Tedesco.

methods capture only the linear relationships between process variables, which perform poorly with regard to fault alarm rates and fault detection rates.

During the past two decades, nonlinear extensions of MSPM methods, such as kernel functions [13], [14] and autoassociative neural networks [15]–[17], have been published in the literature. The kernel PCA method, which was first applied for fault detection by Lee *et al.*, is one of the most commonly adopted nonlinear extensions of PCA [18]. Its basic theory is first to project the original data into a high dimension linear feature space using a kernel function and then to perform corresponding computations in that high dimension linear space. Cui *et al.* [19] proposed improved KPCA from the geometrical viewpoint based on feature vector selection. Alcala and Qin [20] proposed reconstruction-based contributions (RBCs) based on KPCA to identity fault variables. Fezai *et al.* [21] proposed an online reduced KPCA algorithm for monitoring nonlinear dynamic processes. Jiang *et al.* [1] proposed weighted kernel principal component analysis for detecting faults in nonlinear chemical processes. Dhibi *et al.* [22] proposed two nonlinear fault detection methods based on an interval-reduced KPCA for monitoring processes with nonlinear uncertainty. Nonlinear process fault detection based on radial basis kernel mapping has been intensively applied. However, infinite-order nonlinear kernel mapping can be inefficient and redundant. As most industrial processes have dynamic characteristics, Choi and Lee [23] first proposed dynamic principal component analysis (DPCA) for fault detection in nonlinear dynamic processes. Russell *et al.* [2] conducted a comparison study of fault detection methods, PCA, CVA and DPCA; and the CVA model achieved the best sensitivity and promptness.

Very little literature has simultaneously considered nonlinear and dynamic characteristics. Choi and Lee [23] proposed a nonlinear dynamic process monitoring methodology based on dynamic kernel principal component analysis (DKPCA). The simulation results confirmed that DKPCA has the best monitoring performance compared with PCA, DPCA and KPCA. Shang *et al.* [24] proposed a fault detection approach based on the augmented kernel Mahalanobis distance for monitoring nonlinear dynamic processes. Simulation using the Tennessee Eastman process illustrated that the proposed method improves fault detection rates compared with conventional PCA and its variants. Yu and Khan [25] proposed two nonlinear dynamic process fault detection methods based on constructive polynomial mapping (CPM) in which two customized steps are iterated to exponentially increase the order of nonlinear mapping. Two case studies clarified that the proposed methods offer better performance than KICA and DKPCA. Shi *et al.* [26] proposed incipient nonlinear and dynamic fault detection of rolling bearings. Samuel and Cao [27] proposed kernel canonical variate analysis (KCVA) for nonlinear dynamic process monitoring with applications in the TE process. Shang *et al.* [28] extended KCVA to efficient recursive KCVA by introducing the first-order perturbation theory for online fault detection in nonlinear time-varying processes.

A fault alarm will be triggered if at least one monitoring statistic exceeds their corresponding control limits. The essential procedure is subsequently to identify the root reason for the specific fault. Although many studies on fault detection have been published, only a few are related to fault identification. The most popular contribution plot method is usually adopted for diagnosis with the T^2 and Q statistics, which is based on the assumption that related fault variables will cause relatively high contributions. Zhu and Braatz [29] proposed a two-dimensional (2D) contribution map based on the T^2 statistic of PCA for fault identification. Jiang *et al.* [30] proposed CVA-based contributions for identifying associated fault variables based on the variations in both state and residual spaces for offline fault identification. Li *et al.* [31] proposed a canonical variate residual-based fault identification approach to identify the contributions from variables. Shang *et al.* [9] proposed an online fault identification approach based on the exponential weighted moving average to improve the fault identification rates (FIRs) of three types of sensor faults. Lamiaa *et al.* [32] presented a sensor fault diagnosis method based on modified reconstruction-based contributions. Sun *et al.* [33] proposed a probabilistic fault identification method by adopting Bayesian recurrent neural networks. Shang *et al.* [34] proposed an incipient fault diagnosis method for chemical processes based on two-dimensional contribution plots of canonical residual statistics.

Inspired by the abovementioned analysis, we propose a nonlinear and dynamic process fault detection and identification method based on explicit second-order polynomial mapping to overcome the disadvantages of the kernel function method and dynamic characteristics. Four contributions of this paper are presented as follows. First, considering the nonlinear and dynamic characteristics simultaneously, CVA is combined with nonlinear PCA for fault detection and identification in nonlinear dynamic industrial processes. Second, the state vectors are projected into a high-dimensional feature space based on explicit second-order polynomial mapping. Third, the combined statistic Q_c is proposed for detecting the variation in the linear and nonlinear residual space. Finally, a two-dimensional contribution plot based on the combined statistic is given for fault identification. A simulation study of the proposed method compared with PCA, CVA, KPCA, NDPCA [25] and KECA [35] is given in detail, with different faults of the numerical simulation process and the Tennessee Eastman (TE) chemical process.

The remainder of this paper is as follows. Section II briefly reviews the principals of canonical variate analysis and principal component analysis. Section III presents canonical variate nonlinear principal component analysis (CV-NPCA). Section IV provides the detailed steps of the offline and online stages for fault detection and identification in nonlinear dynamic processes. Section V illustrates the monitoring performance of CV-NPCA for nonlinear dynamic processes

with applications in the numerical simulation process and the TE chemical process and provides a comparison study of the fault detection and identification rates of PCA, CVA, KPCA, NDPCA and KECA. The conclusions are presented in Section VI.

II. BRIEF REVIEW OF PRELIMINARY METHODS

A brief description of the relevant methods is reviewed in this section. CVA is introduced as a multivariate statistical analysis approach and followed by a short review of PCA. These two methods serve as the basis of the proposed monitoring method.

A. CANONICAL VARIATE ANALYSIS

CVA is a multivariate statistical analysis approach initially proposed by Hotelling [36]. CVA considers serial correlations by adopting different augmented vectors. The basic theory of CVA is to seek the best linear combinations $a^{\mathrm{T}}y_{f,r}$, $a \in \mathbb{R}^{mp}$ and $b^{\mathrm{T}}y_{p,r}$, $b \in \mathbb{R}^{mp}$. The correlation $\rho_{fp}(a, b)$ between the combinations is maximized as [11]

$$\rho_{fp}(a,b) = \frac{a^{\mathrm{T}}\Sigma_{fp}b}{\left(a^{\mathrm{T}}\Sigma_{ff}a\right)^{1/2}\left(b^{\mathrm{T}}\Sigma_{pp}b\right)^{1/2}}. \tag{1}$$

The above optimization problem can be represented as:

$$\begin{aligned} &\max_{u_1,u_2} \quad u_1^{\mathrm{T}}(\Sigma_{ff}^{-1/2}\Sigma_{fp}\Sigma_{pp}^{-1/2})u_2 \\ &s.t. \quad u_1^{\mathrm{T}}u_1 = 1; \quad u_2^{\mathrm{T}}u_2 = 1. \end{aligned} \tag{2}$$

The covariance and cross-covariance matrices of the past and future observations can be calculated using $\Sigma{=}\mathbf{Y}\mathbf{Y}^{\mathrm{T}}/(N-1)$. The past and future Hankel matrices $\mathbf{Y}_p$ and $\mathbf{Y}_f$ are defined as $\mathbf{Y}_p = \left[y_{p,p+1}\ y_{p,p+2}\ \cdots\ y_{p,p+N}\right] \in \mathbb{R}^{mp\times N}$ and $\mathbf{Y}_f = \left[y_{f,p+1}\ y_{f,p+2}\ \cdots\ y_{f,p+N}\right] \in \mathbb{R}^{mp\times N}$, respectively. The past and future observation vectors $y_{p,r}$ and $y_{f,r}$ can be assembled with the past and future measurements, respectively.

The optimization problem can finally be solved by singular value decomposition of the Hankel matrix $\mathbf{H} = \Sigma_{ff}^{-1/2}\Sigma_{fp}\Sigma_{pp}^{-1/2} = \mathbf{U}\Sigma\mathbf{V}^{\mathrm{T}}$. The state variables $x_r = \mathbf{J}_x y_{p,r} = \mathbf{V}_x\Sigma_{pp}^{-1/2}y_{p,r}$ are a subset of the canonical variates. The prediction errors are represented by $e_r = (\mathbf{I} - \mathbf{V}_x\mathbf{V}_x^{\mathrm{T}})\Sigma_{pp}^{-1/2}y_{p,r}$.

B. PRINCIPAL COMPONENT ANALYSIS

PCA is a classical dimension reduction technique for linear data in which the original data space is decomposed into two subspaces. One is the principal component space representing the dominating variance changes of the data; and the other is the projected space containing variables with small variances, which are usually assumed to be noise. This is only true when the data from industrial processes contain linear features [37]. Mathematically, given a data matrix with n samples of m variables $\mathbf{X} \in \mathbb{R}^{n\times m}$, which have zero means and unit variances, the PCA decomposition can be represented by

$$\mathbf{X} = \mathbf{T}\mathbf{P}^{\mathrm{T}} = \sum_{i=1}^{k}(t_i p_i^{\mathrm{T}}) + \mathbf{E}, \tag{3}$$

where p_i and t_i are the loading vector and the score vector in the PCA model, respectively. Matrix $\mathbf{E}$ represents the residual space. k is the number of retained principal components.

III. CANONICAL VARIATE NONLINEAR PRINCIPAL COMPONENT ANALYSIS

A more detailed explanation of the basic principle of PCA and CVA can be found in [2] and [11]. The proposed hybrid nonlinear dynamic fault detection and identification method consists of three phases, as shown in Fig. 1. CVA is adopted to reduce the effect of the dynamic data characteristics in the first phase. In the second phase, the state vectors are projected into a high-dimensional space by explicit second-order polynomial mapping. The third phase selects the first n_p principal components and the remaining components by performing PCA for fault detection and identification. A detailed schematic of CV-NPCA is given as the following steps.

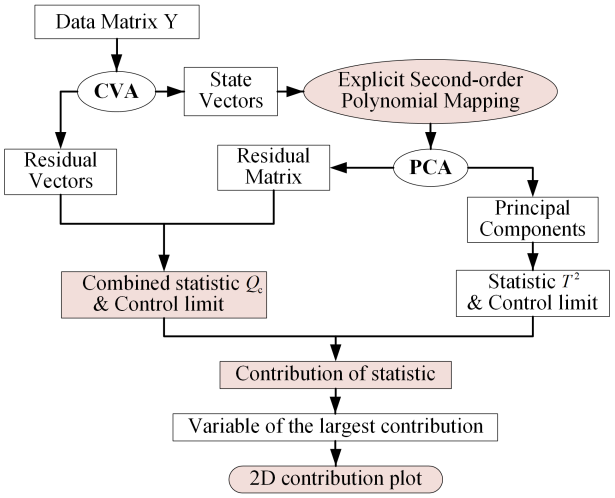

FIGURE 1. Schematic of fault detection and identification based on CV-NPCA.

A. DYNAMIC DATA PREPROCESSED BY CANONICAL VARIATE ANALYSIS

CVA is a linear dimension reduction approach based on multivariate statistical analysis in which the past observation vectors $y_{p,r}$ and future observation vectors $y_{f,r}$ are assembled by the measurement vectors. The measurement vectors are expanded with past and future measurements as

$$y_{p,r} = \begin{bmatrix} y_{r-1} \\ y_{r-2} \\ \vdots \\ y_{r-p} \end{bmatrix} \in \mathbb{R}^{mp}, \quad y_{f,r} = \begin{bmatrix} y_r \\ y_{r+1} \\ \vdots \\ y_{r+p-1} \end{bmatrix} \in \mathbb{R}^{mp}, \tag{4}$$

where r represents a generic index distinguished from the sampling time, p represents the window length of the past and

future observation windows, and y_r is an observation vector from the training data set.

In terms of the equations in [11], let r equal $p+1, p+2, \cdots, p+N$. The Hankel matrices of the past and future observations $\mathbf{Y}_p$ and $\mathbf{Y}_f$ are defined as:

$$\mathbf{Y}_p = \left[y_{p,p+1}\ y_{p,p+2}\ \cdots\ y_{p,p+N}\right] \in \mathbb{R}^{mp\times N}, \tag{5}$$

$$\mathbf{Y}_f = \left[y_{f,p+1}\ y_{f,p+2}\ \cdots\ y_{f,p+N}\right] \in \mathbb{R}^{mp\times N}. \tag{6}$$

Hankel matrices contain $N = l - 2p + 1$ columns. The covariance and cross-covariance matrices can be calculated by using

$$\Sigma_{pp} = \mathbf{Y}_p\mathbf{Y}_p^{\mathrm{T}}/(N-1), \tag{7}$$

$$\Sigma_{ff} = \mathbf{Y}_f\mathbf{Y}_f^{\mathrm{T}}/(N-1), \tag{8}$$

$$\Sigma_{fp} = \mathbf{Y}_f\mathbf{Y}_p^{\mathrm{T}}/(N-1). \tag{9}$$

The solution to the problem of finding the best linear combinations can be obtained by performing SVD on the scaled Hankel matrix.

$$\mathbf{H} = \Sigma_{ff}^{-1/2}\Sigma_{fp}\Sigma_{pp}^{-1/2} = \mathbf{U}\Sigma\mathbf{V}_c^{\mathrm{T}}. \tag{10}$$

The state vectors, which are a part of the estimated canonical variates, are defined as follows:

$$x_r = \mathbf{J}_x y_{p,r} = \mathbf{V}_x\Sigma_{pp}^{-1/2}y_{p,r}, \tag{11}$$

where $\mathbf{V}_x$ includes the first n_c columns of $\mathbf{V}_c$. The number of singular values n_c should be given in advance. The prediction residuals in the scaled past observation space are represented as follows:

$$e_r = \mathbf{F}y_{p,r} = (\mathbf{I} - \mathbf{V}_x\mathbf{V}_x^{\mathrm{T}})\Sigma_{pp}^{-1/2}y_{p,r}. \tag{12}$$

where $\mathbf{I}$ is mp by mp dimensional identity matrix. m means the number of variables. And p denotes the window length of past observation.

B. STATE VECTOR MAPPING BASED ON AN EXPLICIT SECOND ORDER POLYNOMIAL

This subsection introduces state vector mapping based on an explicit second-order polynomial, which can be an efficient alternative to the radial basis kernel method. The detailed second-order polynomial mapping procedure is given as follows:

$$(x_1\ x_2) \xrightarrow{\phi} (x_1\ x_2\ x_1^2\ x_2^2\ x_1x_2). \tag{13}$$

For a two-dimensional vector, the number of mapped state vectors will increase to 5. For a D-dimensional data vector, it should be noted that the mapped state vector has the number of dimensions as follows:

$$P = \frac{D(D+3)}{2}. \tag{14}$$

The subsequent step can reduce the number of dimensions by standard PCA. Specifically, a state vector $x_r \in \mathbb{R}^m$ first undergoes an explicit second-order polynomial mapping to become the mapped state vectors $g_r \in \mathbb{R}^{(m(m+3)/2)}$.

$$g_r = [x_{r1}, \cdots x_{rm}, x_{r1}^2, \cdots x_{rm}^2, x_{r1}x_{r2}, \cdots, x_{r(m-1)}x_{rm}]. \tag{15}$$

After mapping the first n_c state vectors into a high-dimensional space, we can obtain the matrix $\mathbf{G} \in \mathbb{R}^{(N\times(m(m+3)/2)}$ with much fewer nonlinear characteristics.

$$\mathbf{G} = [g_1, g_2, \cdots, g_N]^{\mathrm{T}}. \tag{16}$$

In the mapped latent space, the most significant l-dimensional ($l < D$) latent vectors and $D - l$ dimension residual vectors can be obtained by PCA.

C. PERFORMING PRINCIPAL COMPONENT ANALYSIS

As the subsequent steps for obtaining the matrix $\mathbf{G}$, the standard PCA algorithm is adopted to determine the loading vector and the diagonal matrices $\mathbf{V}$, Λ simultaneously by performing eigenvalue decomposition on the matrix $\mathbf{S}$.

$$\mathbf{S} = \mathbf{G}^{\mathrm{T}}\mathbf{G}/(N_t - 1) = \mathbf{V}\Lambda\mathbf{V}^{\mathrm{T}}, \tag{17}$$

where $\mathbf{V}$ is the loading vector matrix, and Λ is the diagonal matrix $\Lambda = diag(\lambda_1, \lambda_2, \cdots, \lambda_k)$. N_t is the total number of samplings of test data. Matrix $\mathbf{G}$ is expressed as the sum of the product of the loading and score vectors.

$$\mathbf{G} = \mathbf{T}\mathbf{P}^{\mathrm{T}} = \sum_{i=1}^{k}(t_i p_i^{\mathrm{T}}) + \mathbf{E}, \tag{18}$$

where $\mathbf{P}$ represents the first n_p columns of loading vector matrix $\mathbf{V}$, n_p is the number of retained principal elements, p_i is the loading vector, t_i is the score vector in the PCA model, and $\mathbf{E}$ represents the residual matrix. The change direction of the matrix data $\mathbf{G}$ is mainly reflected in the first n_p principal elements. The cumulative contribution rate is generally adopted to choose the number of principal components n_p.

IV. FAULT DETECTION AND IDENTIFICATION BASED ON CV-NPCA

The T^2 statistic and the Q_c combined statistic can be adopted to detect faults for complex industrial processes. The T^2 statistic represents the data variation in the principal component space, which can be calculated according to the following formula with each past observation y_{pp} assembled by the testing fault data set:

$$T^2 = y_{pp}^{\mathrm{T}}\mathbf{P}\Lambda^{-1}\mathbf{P}^{\mathrm{T}}y_{pp}. \tag{19}$$

The Q_c combined statistic reflects the variation of the testing fault data within the nonlinear residual space of CVA and the linear residual space of PCA.

$$Q_c = y_{pp}^{\mathrm{T}}(\mathbf{I} - \mathbf{P}\mathbf{P}^{\mathrm{T}})y_{pp} + e_r^{\mathrm{T}}e_r, \tag{20}$$

where $\mathbf{I}$ is the identity matrix.

The upper control limits of the T^2 and Q_c statistics can be calculated under the assumption that the probability distributions of the state vectors and the residual vectors are Gaussian. If the assumption of a normal distribution does not hold, the probability density function (PDF) is usually adopted by a nonparametric direct estimation approach. Kernel density estimation is the dominant nonparametric method to estimate the PDFs of T^2 and Q_c statistics [8]. Assume that z_1 is a random variable, and $p(z_1)$ denotes the probability density function.

$$P(z_1 < h) = \int_{-\infty}^{h} p(z_1)dz_1. \tag{21}$$

Therefore, if $p(z_1)$ is known, an appropriate control limit can be determined for a specific confidence bound α. The control limits are estimated by replacing $p(z_1)$ with the PDF estimation of the T^2 and Q_c statistics.

$$\int_{-\infty}^{T^2{}_{UCL}} p(T^2)dT^2 = \alpha, \tag{22}$$

$$\int_{-\infty}^{Q_{UCL}} p(Q_c)dQ_c = \alpha. \tag{23}$$

During the online detection process, a fault can be detected when one of the conditions $T^2 > T^2_{UCL}(\alpha)$ or $Q_c > Q_{cUCL}(\alpha)$ is fully satisfied.

After detecting a fault, the urgent work is to find the root reason for the fault. The contributions of the T^2 and Q_c statistics are derived for diagnosis in this section. Considering the contribution based on the residual vectors and principal components from the CV-NPCA model, a 2D variable contribution plot for fault identification was proposed.

Motivated by the contribution of T^2 in [9], the contribution of T^2 and Q_c statistics based on the residual vectors and principal components from the CV-NPCA model can be defined as follows. The contributions of the ith measured variable to statistical index J are denoted by $C^J_{i,k}$, $J \in \{T^2, Q_c, Q_1, Q_2\}$ at time point k.

$$\begin{aligned}\mathbf{C}^{T^2}_{i,k} &= \sum_{j=0}^{p-1} y_{pp}^{\mathrm{T}}\mathbf{P}\Lambda^{-1}\mathbf{V}^{\mathrm{T}}_{(i+mj,1:n_p)}y^{i+mj}_{pp(k)} \\ &= \sum_{j=0}^{p-1} (y^{i+mj}_{pp(k)})^{\mathrm{T}}\mathbf{V}_{(i+mj,1:n_p)}\Lambda^{-1}_{(1:n_p,1:n_p)}\mathbf{V}^{\mathrm{T}}_{(i+mj,1:n_p)}y^{i+mj}_{pp(k)}\end{aligned} \tag{24}$$

where $y^{i+mj}_{pp(k)}$ denotes the $i + mj$ column of y_{pp} at time point k, $\mathbf{V}_{(i+mj,1:n_p)}$ denotes the $i + mj$ row of matrix $\mathbf{V}_{(:,1:n_p)}$, and n_p is the number of principal components from PCA.

$$\mathbf{C}^{Q_c}_{i,k} = \mathbf{C}^{Q_1}_{i,k} + \mathbf{C}^{Q_2}_{i,k} \tag{25}$$

$$\mathbf{C}^{Q_1}_{i,k} = \sum_{j=0}^{p-1} C_{i,j,k}C^{\mathrm{T}}_{i,j,k} \tag{26}$$

$$\begin{aligned}C_{i,k,j} &= (y^{i+mj}_{pp(k)})^{\mathrm{T}}\mathbf{V}_{(i+mj,1:n_p)}(\mathbf{I}_{n_p} - \mathbf{V}^{\mathrm{T}}_{(i+mj,1:n_p)}\mathbf{V}_{(i+mj,1:n_p)}) \\ \mathbf{C}^{Q_2}_{i,k} &= \sum_{j=0}^{p-1} y^{i+mj}_{pp(k)}\mathbf{F}_{(i+mj,:)}(y^{i+mj}_{pp(k)}\mathbf{F}_{(i+mj,:)})^{\mathrm{T}}\end{aligned} \tag{27}$$

where $\mathbf{F}_{(i+mj,:)}$ denotes the $i + mj$ row of matrix $\mathbf{F}$. $\mathbf{I}_{n_p}$ is the identity matrix with n_p dimensions.

For an objective comparison, the contribution indices $\mathbf{C}^{T^2}_{i,k}$ and $\mathbf{C}^{Q_c}_{i,k}$ should be calculated using min-max normalization for each variable. The 2D contribution plot of the T^2 and Q_c statistics is shown in different colors.

The offline training and online detection and identification of the proposed approach can be summarized in the following detailed steps:

Offline Training

1) Set the initial value of p and collect the data $\mathbf{Y} \in \mathbb{R}^{m\times l}$. The order of system n_c should also be given in advance.
2) Assemble matrices $\mathbf{Y}_p$ and $\mathbf{Y}_f$ using formulas (5) and (6), respectively.
3) Calculate the cross-covariance and covariance using formulas (7)-(9).
4) Decompose matrix $\mathbf{H}$ by SVD using formula (10).
5) Compute the state and residual vectors using formulas (11) and (12), respectively.
6) Project the state vectors using an explicit second-order polynomial using formulas (15) and (16).
7) Calculate n_p principal components by eigenvalue decomposition using formulas (17) and (18).
8) Calculate the T^2 statistic, Q_c combined statistic and their corresponding control limits using formulas (19)-(23). If $T^2 > T^2_{UCL}(\alpha)$ or $Q_c > Q_{cUCL}(\alpha)$, then a fault exists.

Online fault detection and identification

1) Obtain measurements at sample time $2p$ and assemble the past observation vector y_{pp}.
2) Calculate the monitoring statistic T^2 and the combined statistic Q_c using formulas (19) and (20), respectively.
3) If the monitoring statistics do not exceed their corresponding control limits, the process operates normally. If the monitoring statistics $T^2 > T^2_{UCL}(\alpha)$ or $Q_c > Q_{cUCL}(\alpha)$, then a fault exists.
4) After a fault is detected, the 2D contributions of statistics can be calculated by formulas (24) and (25).
5) Subsequently, the number of variables with the largest contribution is identified.
6) Finally, the 2D contribution figures are intuitively plotted to diagnose the root reason.

In summary, the entire flowchart of the CV-NPCA procedure for fault detection and identification in nonlinear dynamic processes is given in Fig. 2. First, offline training obtains the projection matrices and the upper control limits. Second, online detection and identification, in which the continuous collection $p+f$ samples are recursively performed as a moving window, are used to check whether the process is

TABLE 1. Comparison of FDRs and FARs (%) in a numerical case.

	Parameter	PCA		KPCA		CVA		NDPCA		KECA		CV-NPCA	
Case		T^2	Q	T^2	Q	T^2	Q	T^2	Q	T^2	Q_c	T^2	Q_c
Actuator additive fault	$f = 0.25$	57.6	1.01	**58.4**	0.40	0.40	60.2	1.92	6.97	55.7	59.5	27.8	**60.2**
Sensor precision degradation	$\delta_e = 0.08$	39.3	0.8	17.6	16.5	**52.4**	43.8	0.8	1.11	14.6	0.81	1.11	**55.3**
FARs													
Normal		1.01	1.01	1.41	0.61	0.51	0.51	0.81	0.51	0.41	0.71	0.51	0.81

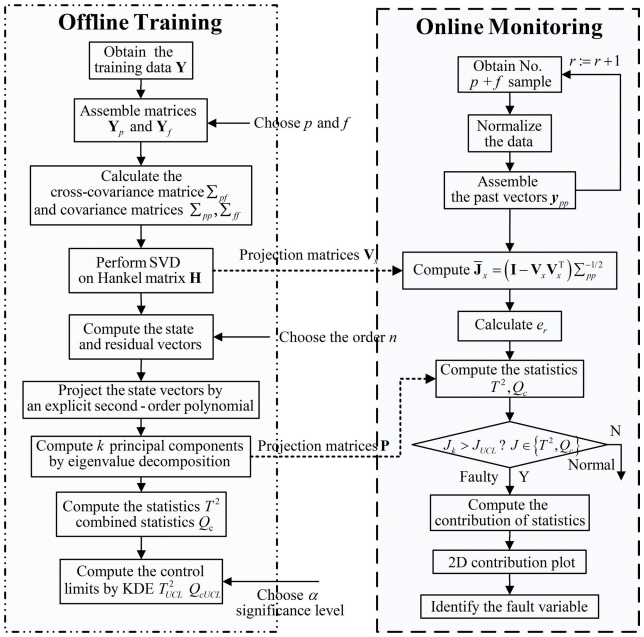

FIGURE 2. Flowchart of CV-NPCA for fault monitoring and identification.

normal. p, f respectively represent the window length of the past and future observation.

V. SIMULATION STUDY

To verify the performance and effectiveness of the proposed fault detection and identification method, a numerical simulation process and the Tennessee Eastman chemical process are adopted.

A. NUMERICAL SIMULATION

A numerical simulation process, which is a five-dimensional nonlinear dynamic system, is considered to generate the training and fault datasets. The model can be formulated as follows [24]:

$$x_{(k+1)} = f[x_{(k)}] + g[u_{(k)}] + w_{(k)}, \tag{28}$$

$$y_k = h[x_{(k)}] + e_{(k)}, \tag{29}$$

where $u = [u_1\ u_2]^{\mathrm{T}}$ and $y = [y_1 \cdots y_4]^{\mathrm{T}}$ represent the inputs and outputs, respectively; and k and $x = [x_1 \cdots x_5]^{\mathrm{T}}$ denote the sampling time and system state, respectively. The mapping functions f, g, h are given as follows:

$$f_{(x)} = \begin{bmatrix} 0.67x_1 - 0.27x_2x_3 + 0.14x_4^2 0.17x_4x_5 \\ -0.24x_1x_2 - 0.45x_2 + 0.14x_3x_4 + 0.11x_4 \\ 0.17x_1 - 0.31x_3 + 0.26x_4 + 0.04x_1x_5 \\ 0.12x_1 - 0.07x_2x_3 - 0.66x_4 + 0.03x_5^2 \\ -0.26x_1 - 0.14x_2 + 0.16x_4 + 0.21x_5^2 \end{bmatrix} \tag{30}$$

$$g_{(x)} = \begin{bmatrix} 1.21x_1 + 0.67x_2 + 0.25x_3^3 \\ 0.95x_2 + 0.33x_3 + 0.32x_5 \\ 0.23x_2^2 + 1.03x_3 + 0.26x_4 \\ 0.94x_1 + 0.21x_4 + 0.47x_5 \end{bmatrix} \tag{31}$$

and

$$h_{(x)} = \begin{bmatrix} 0.26u_1 + 0.93u_2 \\ 2.45u_1 + 0.34u_2^2 \\ 0.28u_1^2 + 0.25u_2^2 \\ 0.37u_1^2 + 0.31u^2 \\ 0.56u_1 + 0.05u_2^3 \end{bmatrix}. \tag{32}$$

In the two formulas (28) and (29), w and e denote Gaussian white noise with standard deviations of $[0.03; 0.03; 0.04; 0.04; 0.03]^{\mathrm{T}}$ and $[0.06; 0.04; 0.06; 0.08]^{\mathrm{T}}$, respectively. The initial state satisfies $x_{(1)} = [1.319; 0.706; 0.438; 0.213; 0.025]^{\mathrm{T}}$. The training dataset contains 400 normal samples. The testing dataset considers the following two types of faults.

1) Actuator additive faults: $u = u^* + f$.

2) Sensor precision degradation: $x = x^* + e$.

Assume that sensor faults occur at x_1 and actuator faults occur at u_1. All of the testing datasets contain 1000 samples, and faults are introduced at the 401st sampling instant and remain until the end. Several methods, such as PCA, CVA, KPCA, NDPCA [25] and KECA [35], have been adopted; and their fault detection rates (FDRs) and fault alarm rates (FARs) are compared. A 90% CPV is used to determine the number of principal components. For NDPCA and CV-NPCA, the maximum time lag is set as 2. The control limits of all the mentioned detection methods are determined by the kernel density estimation method with a 99% confidence level.

In the monitoring charts of Fig. 3, only CV-NPCA and KECA detected the faults simultaneously. However, the Q_c statistic of CV-NPCA has a relatively higher FDR than that of Q from KECA. The 2D contribution plots used to identify actuator fault variables are plotted in Fig. 4. The comparison in Table 1 obviously shows that the CV-NPCA method not only has higher FDRs for the T^2 and Q_c statistics but also has lower FARs for the statistics than other methods for the two types of faults.

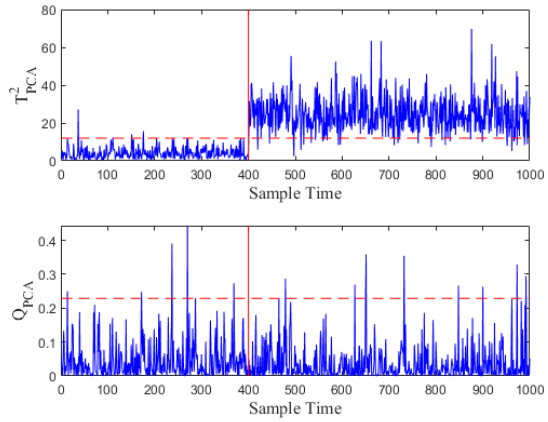

(a) PCA

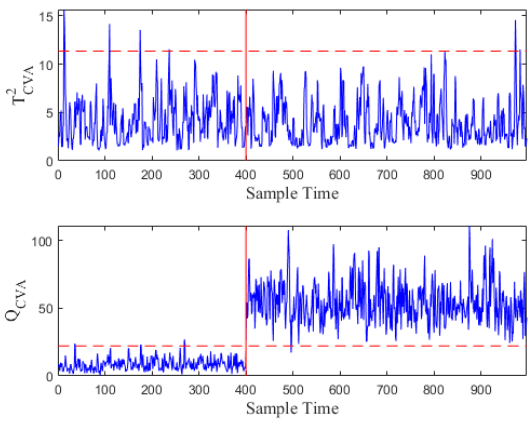

(b) CVA

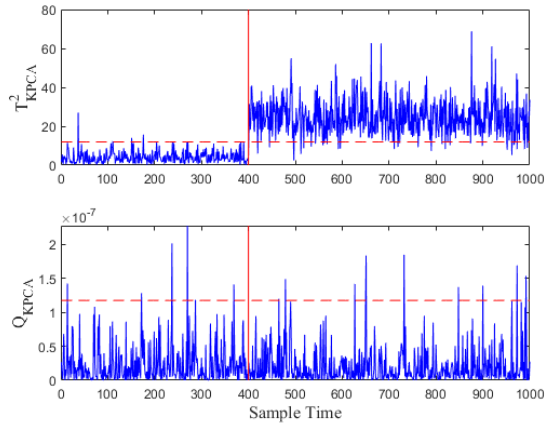

(c) KPCA

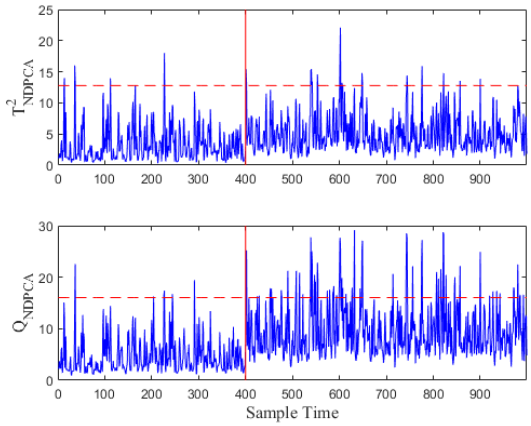

(d) NDPCA

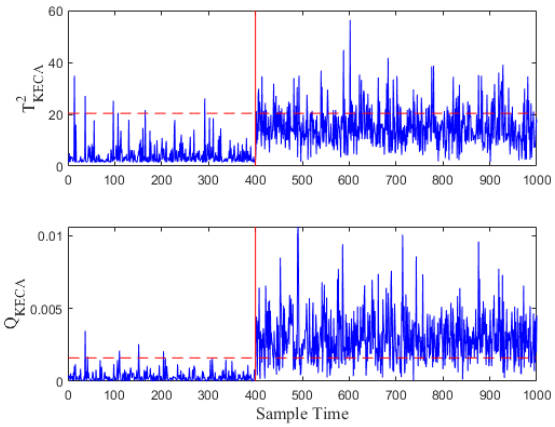

(e) KECA

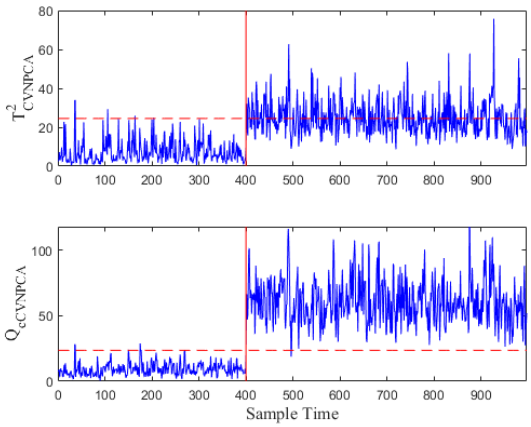

(f) CV-NPCA

FIGURE 3. Monitoring charts of actuator additive faults.

B. TE PROCESS SIMULATION

The schematic of the TE process shown in Fig. 5 consists of five equipment units: a reactor, recycling compressor, vapor-liquid separator, product condenser and product stripper. Two products were produced from four reactants. Additionally, an inert product and a byproduct were also presented for a total of eight components [38]. A distributed control strategy [39] was adopted to make the TE process stable. The relationship among process variables is highly nonlinear because of adopting a decentralized

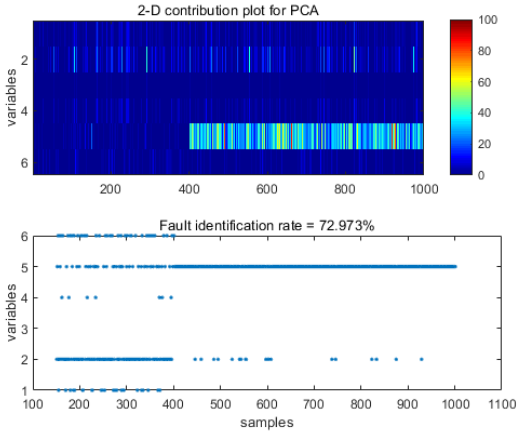

(a) PCA

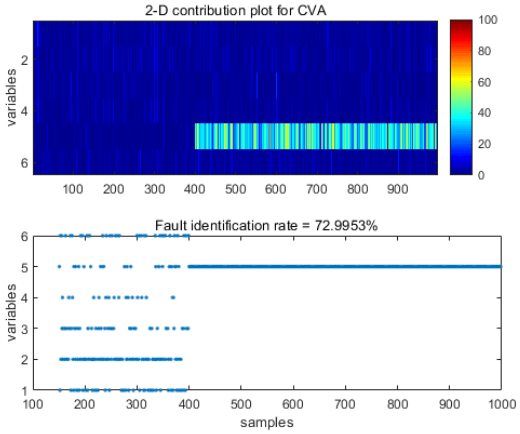

(b) CVA

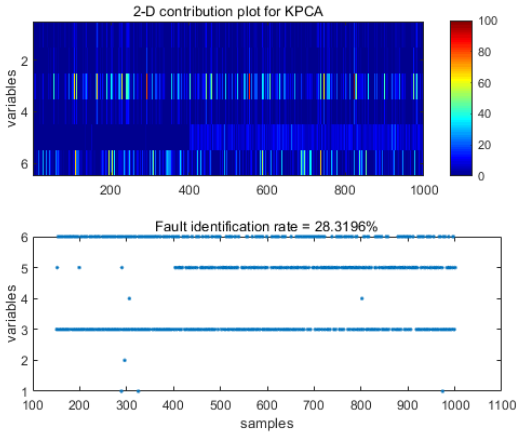

(c) KPCA

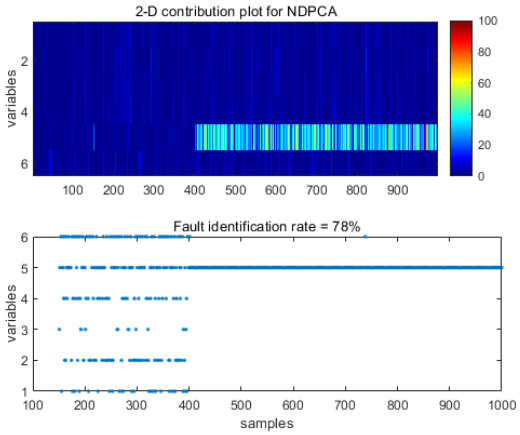

(d) NDPCA

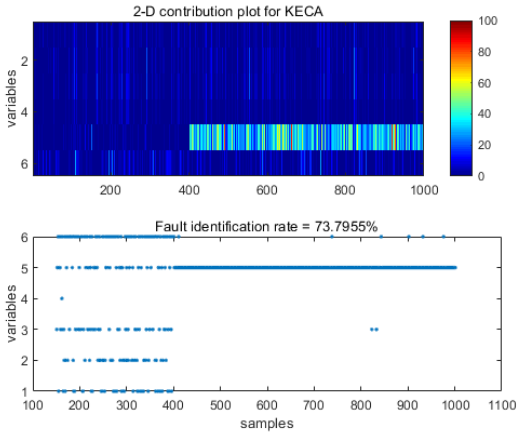

(e) KECA

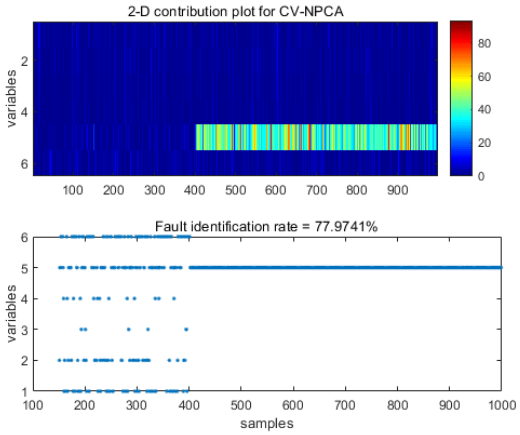

(f) CV-NPCA

FIGURE 4. **Contribution plots of actuator additive faults.**

control strategy. The TE process includes 53 measurements corrupted by additive noise, which are 41 process variables with 12 manipulated variables. In the TE process simulator, the sampling time for most of the variables is 3 minutes. Five variables are sampled every 15 minutes, and 14 variables are sampled at 6-minute intervals [38]. Furthermore, there is strong autocorrelation between process data samples because the recycling of the residual reactants results in dynamic characteristics of the system. In the case study, 16 of the 3-minute sampled process variables are selected for fault

TABLE 2. Selected process variables from the TE process.

No.	Variable	Variable description	Unit
1	XMEAS(1)	A feed (stream 1)	k^3/h
2	XMEAS(2)	D feed (stream 2)	kg/h
3	XMEAS(3)	E feed (stream 3)	kg/h
4	XMEAS(4)	A and C feed (stream 4)	k^3/h
5	XMEAS(5)	Recycle flow (stream 8)	k^3/h
6	XMEAS(6)	Reactor feed rate (stream 6)	k^3/h
7	XMEAS(9)	Reactor temperature	°C
8	XMEAS(10)	Purge rate (stream 9)	k^3/h
9	XMEAS(11)	Separator temperature	°C
10	XMEAS(13)	Separator pressure	kPa gauge
11	XMEAS(14)	Separator underflow (stream 10)	m^3/h
12	XMEAS(16)	Stripper pressure	kPa gauge
13	XMEAS(18)	Stripper temperature	°C
14	XMEAS(19)	Stripper steam flow	kg/h
15	XMEAS(21)	Reactor cooling water outlet temperature	°C
16	XMEAS(22)	Condenser cooling water outlet temperature	°C

TABLE 3. Three types of process faults.

No.	Process variable	Type
Fault(2)	B composition, A/C ratio constant	Step
Fault(11)	Reactor cooling water inlet temperature	Random variation
Fault(19)	Unknown	Unknown

TABLE 4. Parameters used in TE process simulation.

Parameter	PCA	KPCA	CVA	NDPCA	KECA	CV-NPCA
n_{pc}	8	8	8	8	8	8
w_d				2		2
p, f			2			2
c		8000			8000	

detection and identification [25]. These process variables and corresponding descriptions are listed in Table 2.

The TE data blocks include the training and testing data. Each data block includes one normal operation (Fault 0) and 20 fault operations (Fault 1-Fault 20). These 20 faults cover a wide range of fault types, which include step faults, random variations, slow drift, sticking and unknown faults. A brief description of the three types (step, random variation and unknown) of TE faults is given in Table 3 for this case study.

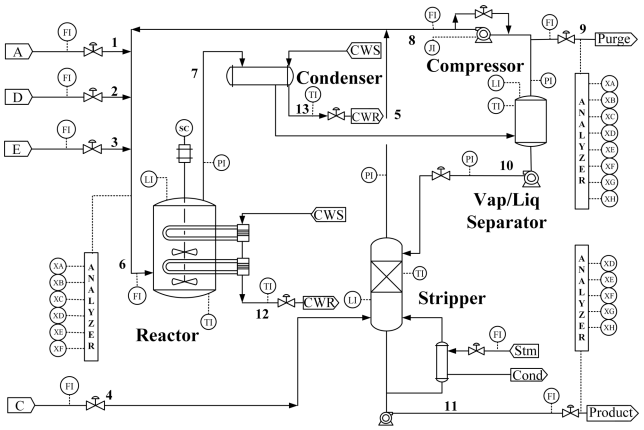

FIGURE 5. The Tennessee Eastman process.

Every testing data block has 960 sampled measurements, and each fault is introduced at the 160th sample time. This means that the TE process is under control before introducing the specific fault. The normal operating data will be assigned as the training data. To compare the monitoring performances impartially, the parameters used in the TE process simulation are listed in Table 4. The width parameter c of the RBF kernel is chosen to be $c = 500 \times m$, as recommended in the literature [18].

C. FAULT 2: B COMPOSITION, A/C RATIO CONSTANT

Fault 2 of the TE process is a step fault in the composition of inert B while the A/C ratio remains constant. The monitoring charts of the statistics generated by PCA, KPCA, CVA, NDPCA, KECA and CV-NPCA are presented in Fig. 6 for further performance comparison. As shown in the figure intuitively, all of the statistics from different approaches successfully detected the step fault. The FARs should be adopted for monitoring performance accurately [36].

TABLE 5. Comparison of FDRs and FARs (%) in the TE process case.

	PCA		KPCA		CVA		NDPCA		KECA		CV-NPCA	
Case	T^2	Q	T^2	Q	T^2	Q	T^2	Q	T^2	Q_c	T^2	Q_c
Fault 1	99.5	**99.8**	**99.7**	99.7	99.5	99.3	99.5	99.6	99.5	99.5	99.4	99.6
Fault 2	97.3	98.4	98.3	98.5	97.3	98.4	97.5	97.6	**98.4**	96.8	**98.1**	**98.6**
Fault 3	**9.8**	3.9	8.9	3.4	9.8	3.6	2.3	**5.6**	3.0	3.6	3.5	5.1
Fault 4	9.26	0.5	**12.1**	1.88	9.26	0.5	10.5	**9.89**	6.88	0.75	9.14	4.88
Fault 5	31.6	20.4	**38.4**	23.5	31.3	18.1	31.4	**32.2**	29.2	21.0	32.9	25.2
Fault 6	99.4	99.4	**99.8**	99.6	99.3	99.4	99.6	99.6	99.3	99.4	99.8	**99.8**
Fault 7	44.7	33.7	46.4	31.8	44.7	32.5	**55.7**	**52.2**	36.7	39.6	50.8	38.7
Fault 8	97.6	96.5	**99.1**	97	97.6	95.5	96.8	97.5	97.8	96.4	98.7	**98**
Fault 9	2.0	1.88	0.5	1.75	2.0	**2.25**	**2.38**	0.5	1.38	0.63	1.75	1.5
Fault 10	55.1	49.2	**85.5**	89.5	54.9	23.8	60.8	60.6	42.2	45.1	64.1	**90.5**
Fault 11	17.2	42.9	13.9	8.26	17.0	37.6	21.0	21.9	35.5	18.9	**46.8**	**61.2**
Fault 12	99	94.9	99.5	98.8	99	89.8	96.6	97.3	**98.6**	97.8	**98.8**	**99.5**
Fault 13	95.2	95.1	95.8	95.5	95.2	95.1	**96.4**	**97.4**	95.1	94.7	95.2	95.1
Fault 14	91.9	99.8	89.6	**99.7**	89.8	99.2	83.6	84.8	96.7	**99.8**	**99.7**	99.7
Fault 15	28.9	6.63	**34.2**	5.26	29.0	6.01	28.0	**30.2**	18.2	6.51	27.0	9.64
Fault 16	24.2	12.0	**41.8**	34.8	23.8	12.5	20.6	21.4	22.0	8.14	18.8	**35.3**
Fault 17	83.4	96.5	88.9	90.5	82.9	91.9	85.8	84.9	82.4	89.6	**94.7**	**97.5**
Fault 18	89.5	90.7	90.2	90.8	89.5	89.9	89.2	89.2	89.8	89.7	**90.2**	**91.0**
Fault 19	17.7	13.6	20.5	76.9	17.6	12.8	1.13	0.75	13.0	13.5	**22.4**	**74.5**
Fault 20	46.2	49.3	**85.8**	70.2	45.9	23.8	47.7	56.9	49.1	32.4	59.9	**74.2**
FARs												
Fault 0	3.60	1.88	**2.50**	2.03	5.63	9.4	9.55	5.79	3.29	0.94	2.97	**0.47**

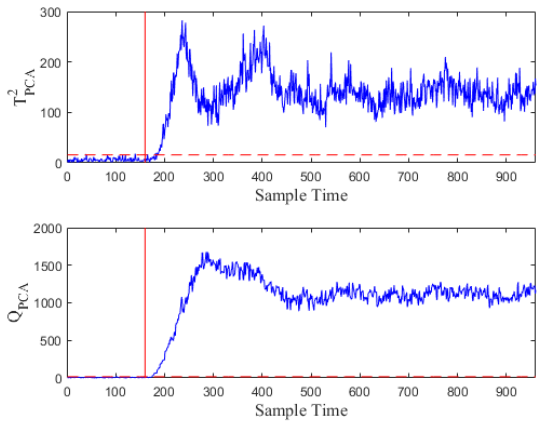

(a) PCA

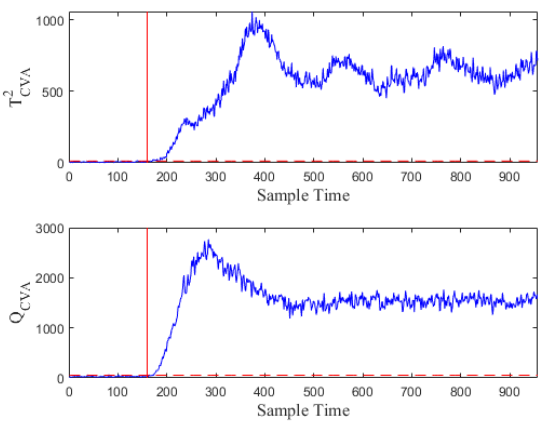

(b) CVA

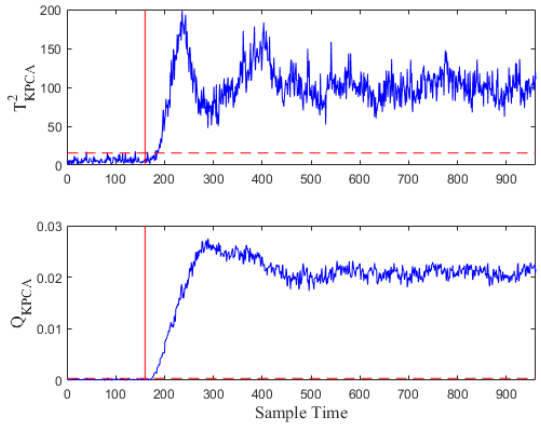

(c) KPCA

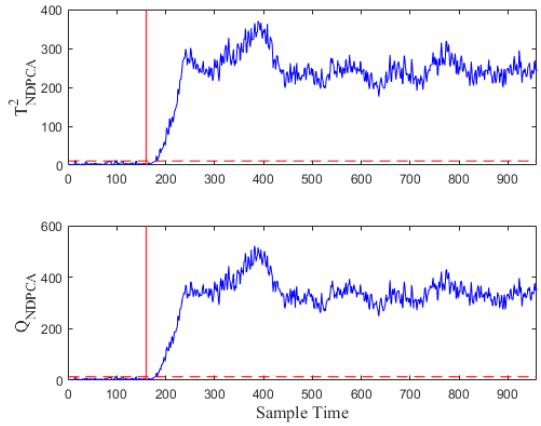

(d) NDPCA

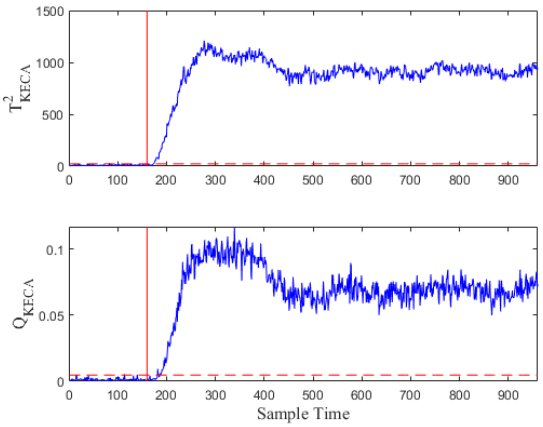

(e) KECA

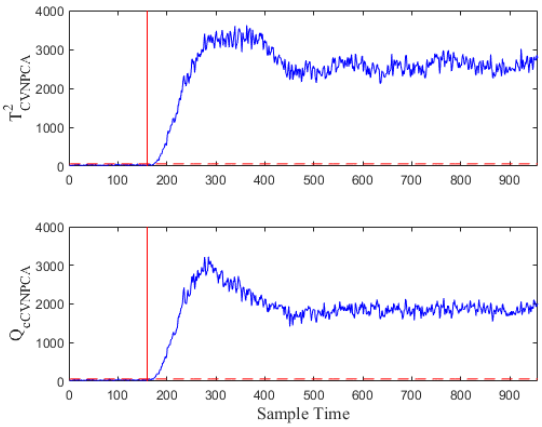

(f) CV-NPCA

FIGURE 6. **Monitoring charts of fault 2.**

A 2D contribution plot is adopted to identify the fault variable. Although all of the contribution plots from the six different approaches in Fig. 7 show correct identification results, they have different FIRs, as shown in the largest contribution variable figure. CV-NPCA has the highest fault identification rate of 98.1459%, which verifies the effectiveness of adopting explicit second-order polynomial mapping. The FIRs from PCA, CVA, and KPCA are less than 98%. Because of employing the kernel function, KPCA has the highest fault identification rate of 97.8996% among those

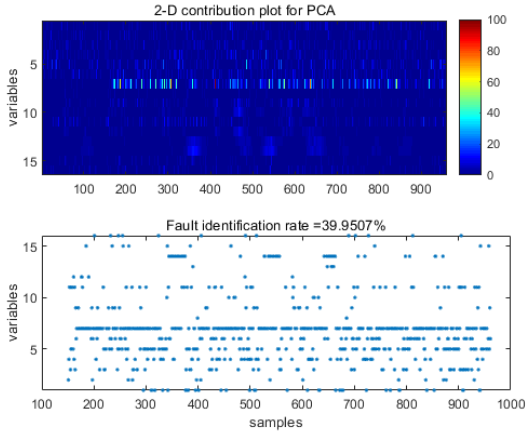

(a) PCA

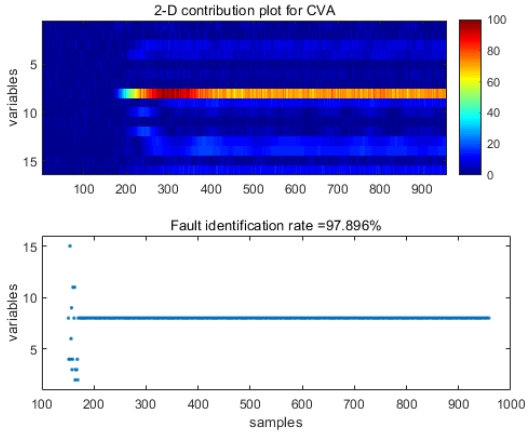

(b) CVA

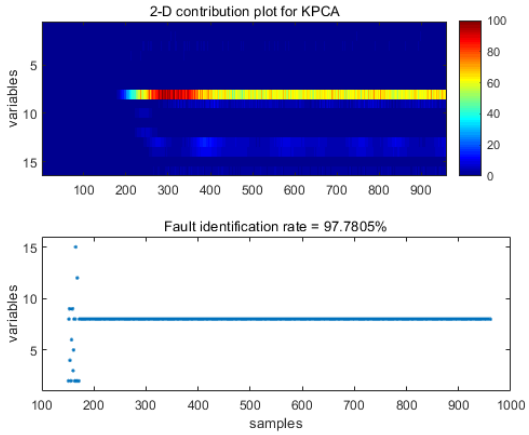

(c) KPCA

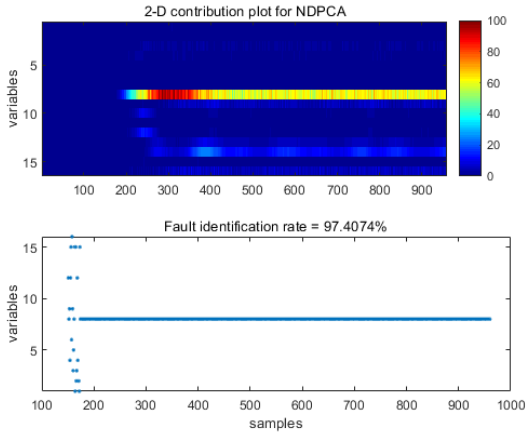

(d) NDPCA

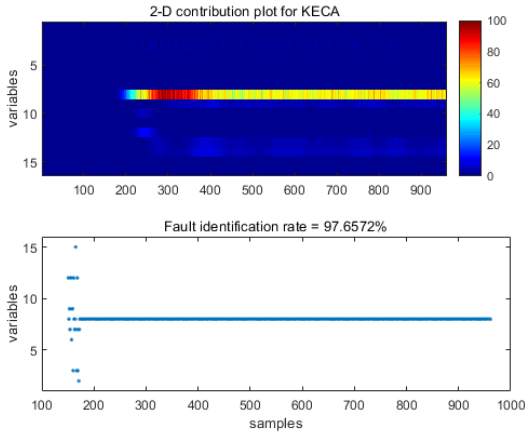

(e) KECA

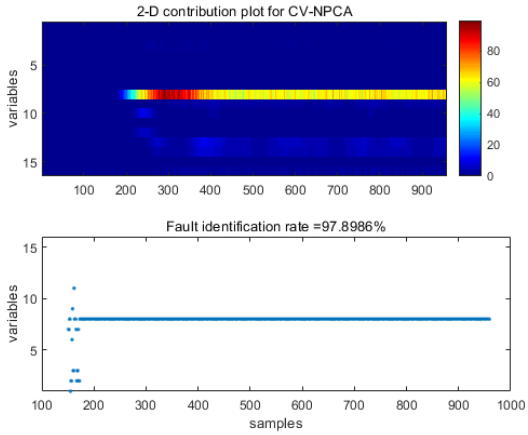

(f) CV-NPCA

FIGURE 7. **Contribution plots of fault 2.**

three methods. A step fault in the composition of inert B causes the purge rate (MXEAS(10)) to increase rapidly. The purge rate (MXEAS(10)) is 8. This result is consistent with the identification results in the largest contribution variable figure.

D. FAULT 11: REACTOR COOLING WATER INLET TEMPERATURE

Fault 11 of the TE process is associated with the reactor cooling water inlet temperature, which is a random variation in the process variable. To further illustrate the performance

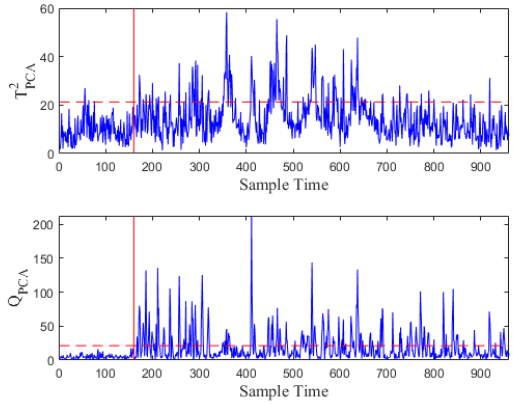

(a) PCA

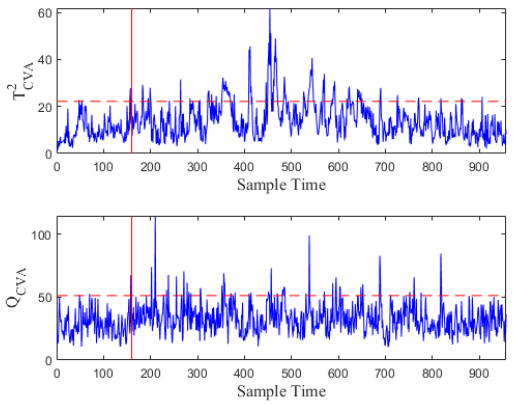

(b) CVA

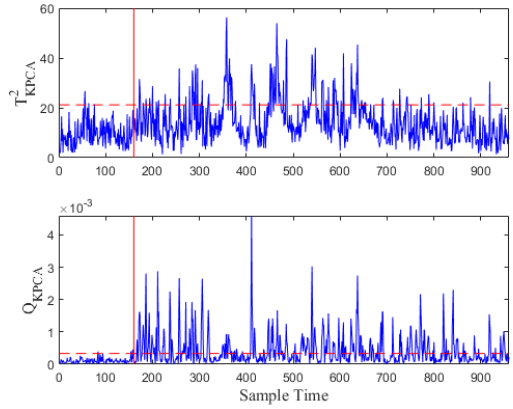

(c) KPCA

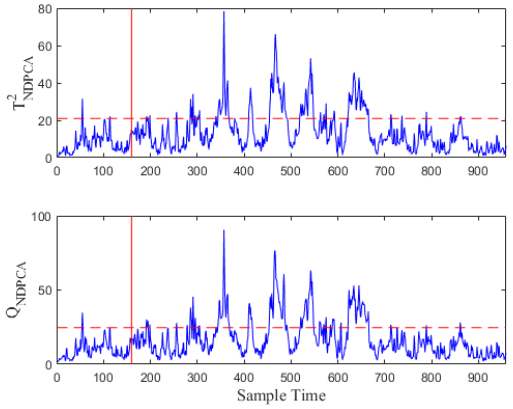

(d) NDPCA

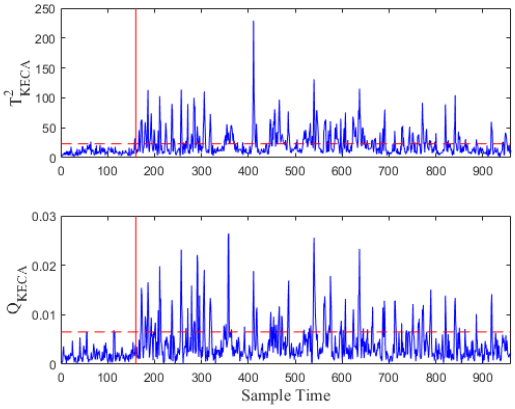

(e) KECA

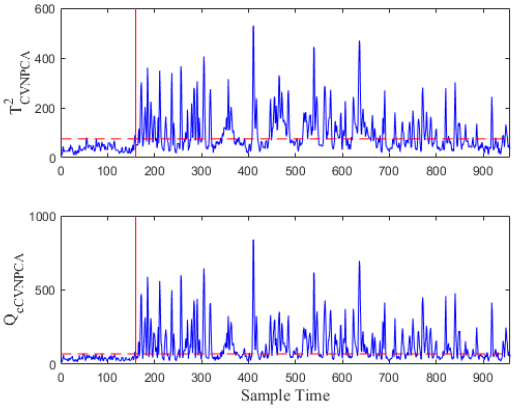

(f) CV-NPCA

FIGURE 8. **Monitoring charts of fault 11.**

comparison, the monitoring charts of the statistics generated by six methods are presented in Fig. 8. It is intuitively observed from the figures that CV-NPCA is more sensitive, especially after the 700th sampling time.

Fault 11 caused a great shock of the cooling water flow rate in the reactor, which made the temperature of the reactor fluctuate. The other variables remain near the set points as in normal operations. However, only 16 variables sampled for 3 minutes are adopted for this case study, and the cooling water flow rate in the reactor is not included in the data set. The most relevant fault variable is the temperature of the reactor (XMEAS(9)). Although all of the contribution plots from different approaches show correct identification results, they have different FIRs, as shown in the largest contribution

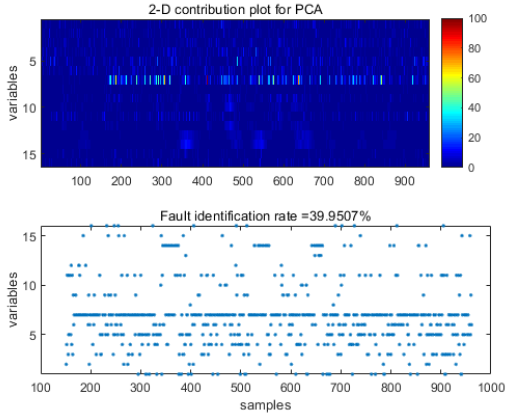

(a) PCA

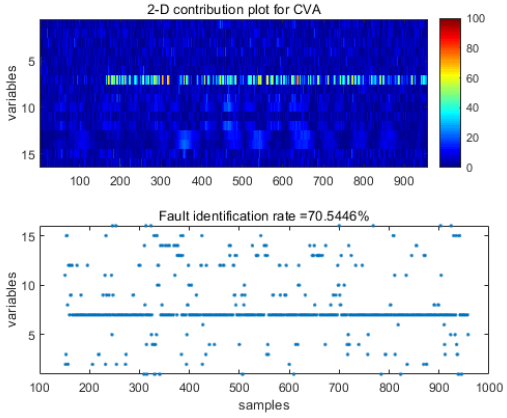

(b) CVA

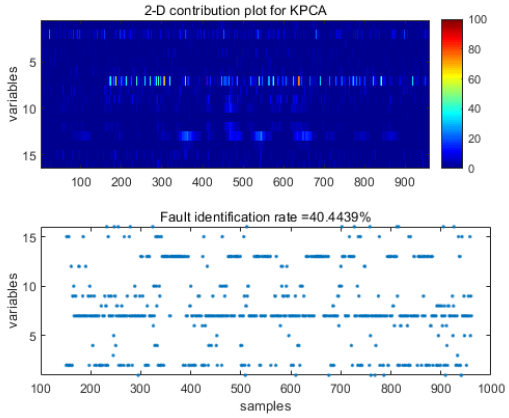

(c) KPCA

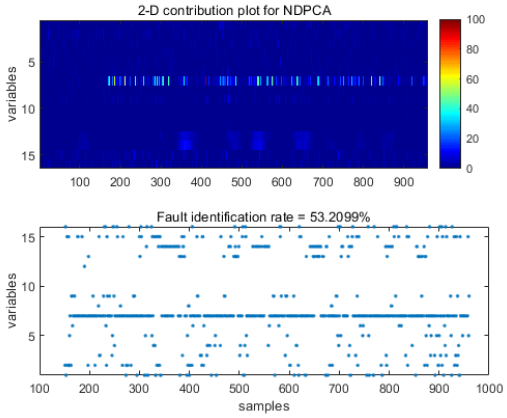

(d) NDPCA

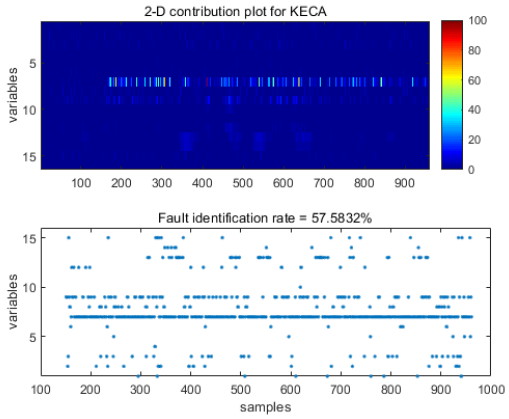

(e) KECA

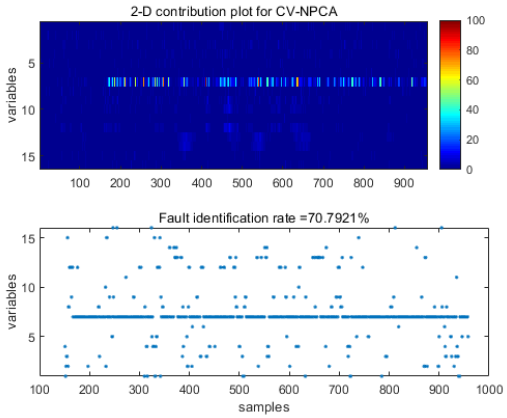

(f) CV-NPCA

FIGURE 9. **Contribution plots of fault 11.**

variable in Fig. 9. CV-NPCA has the highest fault identification rate of 70.7921%, which verifies the effectiveness of adopting explicit second-order polynomial mapping. The FIRs of PCA, KPCA, NDPCA, and KECA are less than 70.5%. PCA has the lowest fault identification rate of 39.9507% among those four methods.

E. FAULT 19: UNKNOWN

The description of fault 19 is unknown according to [40]. It can be observed that the Q_c statistic of CV-NPCA is more sensitive and has the highest FDRs in Fig. 10. The Q statistic of CVA has nearly the same results, as shown in the figure.

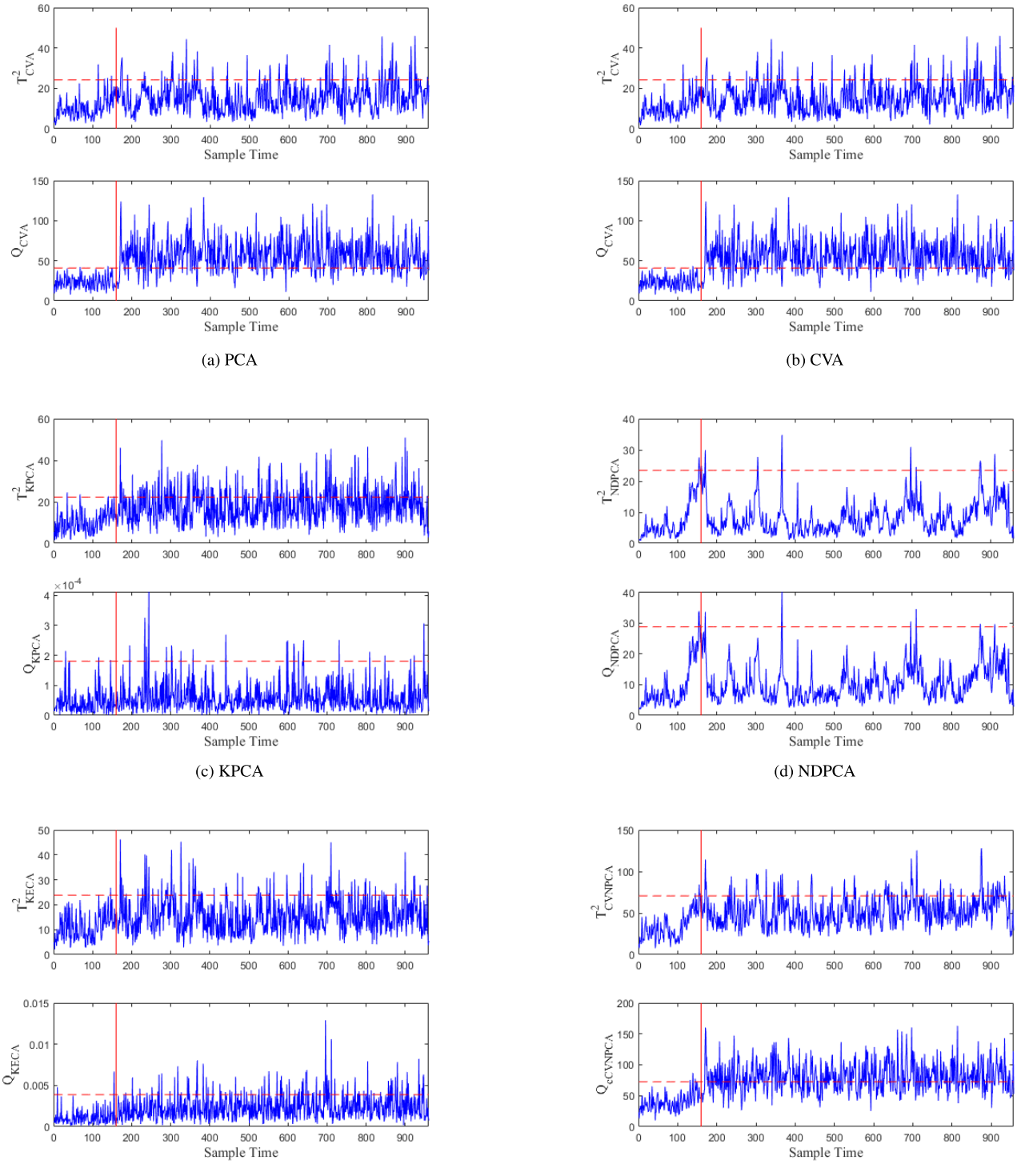

(a) PCA (b) CVA

(c) KPCA (d) NDPCA

(e) KECA (f) CV-NPCA

FIGURE 10. **Monitoring charts of fault 19.**

The specific description of fault 19 is not given. However, it can be observed from the contribution plot from different approaches. Recycle flow (stream 8) (XMEAS(5)) is the root reason for this unknown fault. Although all figures show correct identification results, they have different FIRs, as shown in the largest contribution variable in Fig. 11. CV-NPCA has the highest fault identification rate of 66.2723%, which verifies the effectiveness of adopting explicit second-order polynomial mapping. FIRs from CVA, KPCA, NDPCA, and KECA are less than 60%. KECA has the lowest fault

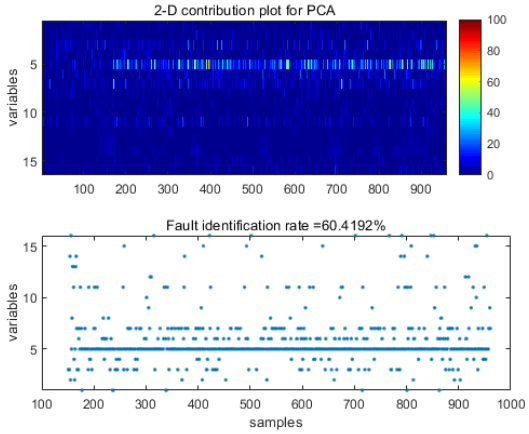

(a) PCA

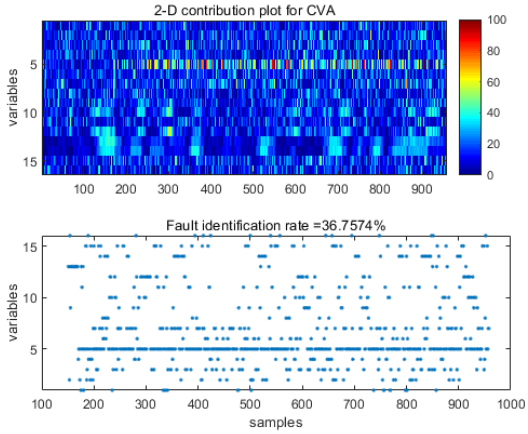

(b) CVA

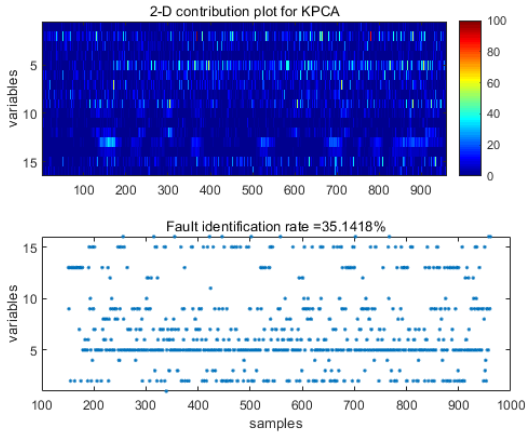

(c) KPCA

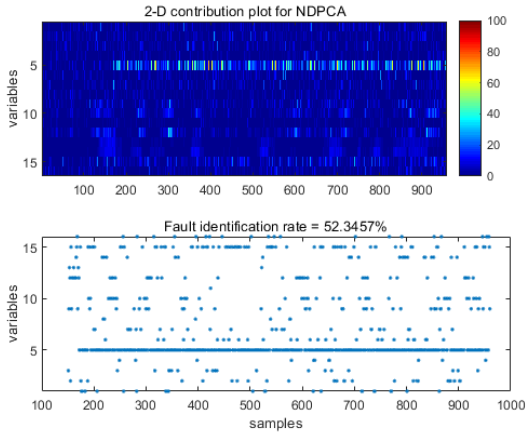

(d) NDPCA

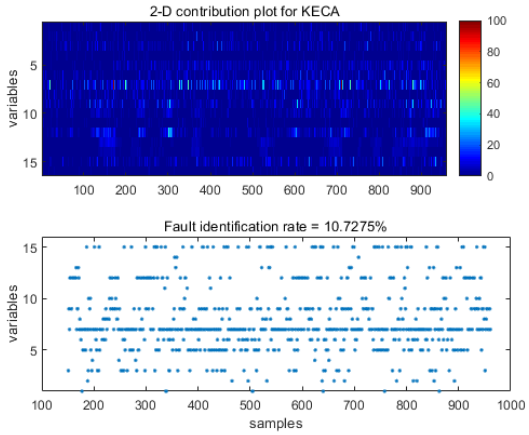

(e) KECA

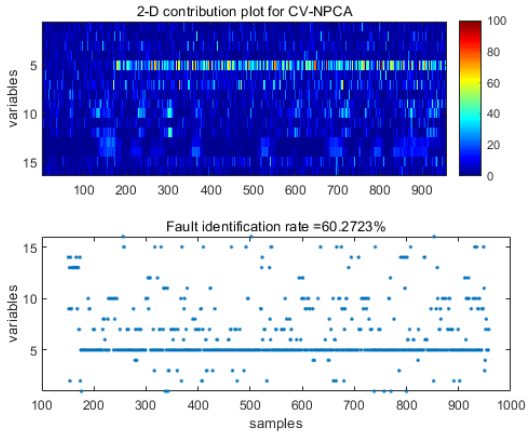

(f) CV-NPCA

FIGURE 11. **Contribution plots of fault 19.**

identification rate of 10.7275% among those four methods. This may be because the parameter of the radial basic function is not optimal in this case study.

Compared with PCA, CVA, KPCA, NDPCA and KECA, Table 5 shows that the proposed CV-NPCA has relatively higher FDRs for T^2 statistics and the Q_c combined statistics for faults 2, 6, 8, 10, 11, 12, 16, 17, 18, and 19. Process faults 3, 4, and 9 are hard to detect, so they are ignored in the discussion. That is, the proposed CV-NPCA can explain much more variance in the principal component and residual

TABLE 6. Detection delay sampling times in the TE process case.

	PCA		KPCA		CVA		NDPCA		KECA		CV-NPCA	
Case	T^2	Q	T^2	Q	T^2	Q	T^2	Q	T^2	Q_c	T^2	Q_c
Fault 1	9	5	16	10	**3**	**3**	8	6	15	9	5	4
Fault 2	17	17	43	**15**	**11**	16	18	18	30	32	16	16
Fault 3	85	UD	UD	UD	84	418	407	22	UD	89	UD	88
Fault 4	73	UD	UD	UD	62	UD	61	62	UD	UD	71	UD
Fault 5	3	3	27	4	3	4	3	3	27	3	**3**	**3**
Fault 6	3	3	36	3	3	3	3	3	31	3	**3**	**3**
Fault 7	3	3	4	3	3	3	3	4	3	3	**3**	**3**
Fault 8	28	23	66	25	10	21	**9**	**9**	66	23	10	22
Fault 9	UD	UD	UD	UD	UD	UD	233	UD	UD	UD	UD	UD
Fault 10	38	50	UD	148	22	23	**16**	**16**	UD	27	21	21
Fault 11	14	12	UD	12	164	198	187	127	UD	13	**11**	**11**
Fault 12	5	5	35	5	4	4	9	4	108	5	**4**	**4**
Fault 13	48	43	94	46	**38**	40	46	47	75	48	41	**40**
Fault 14	6	3	UD	3	4	3	5	3	38	4	**3**	**3**
Fault 15	393	240	UD	580	243	594	396	92	UD	577	392	578
Fault 16	36	196	UD	199	**27**	**23**	40	37	UD	315	37	38
Fault 17	28	22	37	26	26	21	25	25	56	24	25	**21**
Fault 18	91	82	107	87	79	77	90	90	103	87	**83**	**77**
Fault 19	79	UD	UD	UD	14	12	UD	UD	UD	488	**12**	**12**
Fault 20	**82**	89	UD	94	72	76	82	82	UD	92	83	**76**

UD : fault was not successfully detected.

space than the other process monitoring methods. Regarding the rest of the faults, the proposed CV-NPCA has nearly the same performance as that of the compared methods. From the simulation comparison, the proposed method has relatively high sensitivity in most fault cases compared to other methods. The detection delay sampling time presented in Table 6 is calculated as the difference between the fault starting sampling time and the fault detection sampling time.

While the statistics exceeded the control limit at three consecutive sampling moments, the fault detection time can be identified. CV-NPCA has relatively lower FARs than other methods. In particular, the Q_c statistic of CV-NPCA have the lowest FAR.

VI. CONCLUSION

To improve the effectiveness of traditional approaches in monitoring nonlinear dynamic processes, a fault detection and identification approach based on explicit second-order polynomial mapping and combined statistic is proposed. Training data are first preprocessed by adopting different augmented vectors from CVA to eliminate the strong serial correlation among variables. Then, state vectors are projected by explicit second-order polynomial mapping into a higher dimensional feature space. Finally, the n_p principal components and residual vectors are obtained by conventional PCA for online monitoring. The combined statistic Q_c is proposed for monitoring the variation in both nonlinear and linear residual spaces. The corresponding upper control limits are calculated based on probability density estimation. This approach is applied to a numerical simulation and the TE chemical process for fault detection and identification. Compared to the simulation results of PCA, CVA, KPCA, NDPCA and KECA, the proposed CV-NPCA can effectively reduce the adverse effect from the nonlinear and dynamic characteristics of industrial process data. The proposed method can obtain not only much higher FDRs but also relatively higher FIRs. An approach for incipient fault detection and diagnosis will be further investigated based on combining CVA with PCA.

REFERENCES

[1] Q. Jiang and X. Yan, "Weighted kernel principal component analysis based on probability density estimation and moving window and its application in nonlinear chemical process monitoring," *Chemometrics Intell. Lab. Syst.*, vol. 127, pp. 121–131, Aug. 2013.

[2] E. L. Russell, L. H. Chiang, and R. D. Braatz, "Fault detection in industrial processes using canonical variate analysis and dynamic principal component analysis," *Chemometrics Intell. Lab. Syst.*, vol. 51, no. 1, pp. 81–93, 2000.

[3] D. Garcia-Alvarez, M. J. Fuente, and G. I. Sainz, "Fault detection and isolation in transient states using principal component analysis," *J. Process Control*, vol. 22, no. 3, pp. 551–563, Mar. 2012.

[4] X. Wang, U. Kruger, and B. Lennox, "Recursive partial least squares algorithms for monitoring complex industrial processes," *Control Eng. Pract.*, vol. 11, no. 6, pp. 613–632, Jun. 2003.

[5] Y. Zhang, Y. Teng, and Y. Zhang, "Complex process quality prediction using modified kernel partial least squares," *Chem. Eng. Sci.*, vol. 65, no. 6, pp. 2153–2158, Mar. 2010.

[6] Q. Jia and Y. Zhang, "Quality-related fault detection approach based on dynamic kernel partial least squares," *Chem. Eng. Res. Des.*, vol. 106, pp. 242–252, Feb. 2016.

[7] B. C. Juricek, D. E. Seborg, and W. E. Larimore, "Fault detection using canonical variate analysis," *Ind. Eng. Chem. Res.*, vol. 43, no. 2, pp. 458–474, 2004.

[8] P.-E. P. Odiowei and Y. Cao, "Nonlinear dynamic process monitoring using canonical variate analysis and kernel density estimations," *IEEE Trans. Ind. Informat.*, vol. 6, no. 1, pp. 36–45, Feb. 2010.

[9] L. Shang, J. Liu, and Y. Zhang, "Recursive fault detection and identification for time-varying processes," *Ind. Eng. Chem. Res.*, vol. 55, no. 46, pp. 12149–12160, Nov. 2016.

[10] Y. Zhang, S. Li, and Y. Teng, "Dynamic processes monitoring using recursive kernel principal component analysis," *Chem. Eng. Sci.*, vol. 72, pp. 78–86, Apr. 2012.

[11] L. Shang, J. Liu, K. Turksoy, Q. M. Shao, and A. Cinar, "Stable recursive canonical variate state space modeling for time-varying processes," *Control Eng. Pract.*, vol. 36, pp. 113–119, Mar. 2015.

[12] C. Chakour, M.-F. Harkat, and M. Djeghaba, "Neuronal principal component analysis for nonlinear time-varying processes monitoring," *IFAC-PapersOnLine*, vol. 48, no. 21, pp. 1408–1413, 2015.

[13] B. Schölkopf, A. Smola, and K.-R. Müller, "Kernel principal component analysis," in *Proc. Int. Conf. Artif. Neural Netw.* London, U.K.: Springer, 1997, pp. 583–588.

[14] V. H. Nguyen and J.-C. Golinval, "Fault detection based on kernel principal component analysis," *Eng. Struct.*, vol. 32, no. 11, pp. 3683–3691, Nov. 2010.

[15] M. A. Kramer, "Nonlinear principal component analysis using autoassociative neural networks," *AIChE J.*, vol. 37, no. 2, pp. 233–243, Feb. 1991.

[16] D. Dong and T. J. McAvoy, "Nonlinear principal component analysis—Based on principal curves and neural networks," *Comput. Chem. Eng.*, vol. 20, no. 1, pp. 65–78, 1996.

[17] F. Jia, E. B. Martin, and A. J. Morris, "Non-linear principal components analysis with application to process fault detection," *Int. J. Syst. Sci.*, vol. 31, no. 11, pp. 1473–1487, Jan. 2000.
[18] J.-M. Lee, C. K. Yoo, S. W. Choi, P. A. Vanrolleghem, and I.-B. Lee, "Nonlinear process monitoring using kernel principal component analysis," *Chem. Eng. Sci.*, vol. 59, no. 1, pp. 223–234, Jan. 2004.
[19] P. Cui, J. Li, and G. Wang, "Improved kernel principal component analysis for fault detection," *Expert Syst. Appl.*, vol. 34, no. 2, pp. 1210–1219, Feb. 2008.
[20] C. F. Alcala and S. J. Qin, "Reconstruction-based contribution for process monitoring with kernel principal component analysis," *Ind. Eng. Chem. Res.*, vol. 49, no. 17, pp. 7849–7857, Sep. 2010.
[21] R. Fezai, M. Mansouri, O. Taouali, M. F. Harkat, and N. Bouguila, "Online reduced kernel principal component analysis for process monitoring," *J. Process Control*, vol. 61, pp. 1–11, Jan. 2018.
[22] K. Dhibi, R. Fezai, M. Mansouri, A. Kouadri, M.-F. Harkat, K. Bouzara, H. Nounou, and M. Nounou, "A hybrid approach for process monitoring: Improving data-driven methodologies with dataset size reduction and interval-valued representation," *IEEE Sensors J.*, vol. 20, no. 17, pp. 10228–10239, Sep. 2020.
[23] S. W. Choi and I. B. Lee, "Nonlinear dynamic process monitoring based on dynamic kernel PCA," *Chem. Eng. Sci.*, vol. 59, no. 24, pp. 5897–5908, 2004.
[24] J. Shang, M. Chen, and H. Zhang, "Fault detection based on augmented kernel Mahalanobis distance for nonlinear dynamic processes," *Comput. Chem. Eng.*, vol. 109, pp. 311–321, Jan. 2018.
[25] H. Yu and F. Khan, "Improved latent variable models for nonlinear and dynamic process monitoring," *Chem. Eng. Sci.*, vol. 168, pp. 325–338, Aug. 2017.
[26] H. Shi, J. Guo, X. Bai, L. Guo, Z. Liu, and J. Sun, "Research on a nonlinear dynamic incipient fault detection method for rolling bearings," *Appl. Sci.*, vol. 10, no. 7, p. 2443, 2020.
[27] R. T. Samuel and Y. Cao, "Kernel canonical variate analysis for nonlinear dynamic process monitoring," *IFAC-PapersOnLine*, vol. 48, no. 8, pp. 605–610, 2015.
[28] L. Shang, J. Liu, and Y. Zhang, "Efficient recursive kernel canonical variate analysis for monitoring nonlinear time-varying processes," *Can. J. Chem. Eng.*, vol. 96, no. 1, pp. 205–214, Jan. 2018.
[29] X. Zhu and R. D. Braatz, "Two-dimensional contribution map for fault identification [focus on education]," *IEEE Control Syst. Mag.*, vol. 34, no. 5, pp. 72–77, 2014.
[30] B. Jiang, D. Huang, X. Zhu, F. Yang, and R. D. Braatz, "Canonical variate analysis-based contributions for fault identification," *J. Process Control*, vol. 26, pp. 17–25, Feb. 2015.
[31] X. Li, X. Yang, Y. Yang, I. Bennett, A. Collop, and D. Mba, "Canonical variate residuals-based contribution map for slowly evolving faults," *J. Process Control*, vol. 76, pp. 87–97, Apr. 2019.
[32] L. M. Elshenawy and T. A. Mahmoud, "Fault diagnosis of time-varying processes using modified reconstruction-based contributions," *J. Process Control*, vol. 70, pp. 12–23, Oct. 2018.
[33] W. Sun, A. R. C. Paiva, P. Xu, A. Sundaram, and R. D. Braatz, "Fault detection and identification using Bayesian recurrent neural networks," *Comput. Chem. Eng.*, vol. 141, Oct. 2020, Art. no. 106991.
[34] L. Shang, Z. Lu, C. Wen, and A. Qiu, "Canonical residual based incipient fault detection and diagnosis for chemical process," *Control Theory Appl.*, vol. 38, no. 8, pp. 1247–1256, 2021.
[35] R. Jenssen, "Kernel entropy component analysis," *IEEE Trans. Pattern Anal. Mach. Intell.*, vol. 32, no. 5, pp. 847–860, May 2010.
[36] L. Shang, J. Liu, Y. Zhang, and G. Wang, "Efficient recursive canonical variate analysis approach for monitoring time-varying processes," *J. Chemometrics*, vol. 31, no. 1, Jan. 2017, Art. no. e2858.
[37] X. Deng, X. Tian, S. Chen, and C. J. Harris, "Nonlinear process fault diagnosis based on serial principal component analysis," *IEEE Trans. Neural Netw. Learn. Syst.*, vol. 29, no. 3, pp. 560–572, Mar. 2018.
[38] L. H. Chiang, R. D. Braatz, and E. Russell, *Fault Detection and Diagnosis in Industrial Systems*. London, U.K.: Springer, 2001.
[39] P. R. Lyman and C. Georgakis, "Plant-wide control of the Tennessee Eastman problem," *Comput. Chem. Eng.*, vol. 19, no. 3, pp. 321–331, Mar. 1995.
[40] L. H. Chiang, E. L. Russell, and R. D. Braatz, *Fault Detection and Diagnosis in Industrial Systems*. London, U.K.: Springer, 2000.

LIANGLIANG SHANG was born in Zibo, Shandong, China, in 1981. He received the M.E. degree in control theory and control engineering from the Shandong University of Science and Technology, Qingdao, China, in 2010, and the Ph.D. degree in control theory and control engineering from Northeastern University, Shenyang, China, in 2016. He is currently a Lecturer with the School of Electrical Engineering, Nantong University. His research interests include complex industrial process modeling, fault detection, and diagnosis.

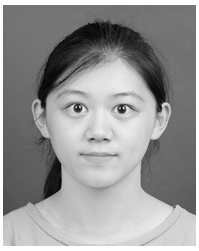

KEXIN SHI received the B.E. degree in electrical engineering and automation from Nantong University, Nanjing, China, in 2021, where she is currently pursuing the M.S. degree in control theory and control engineering. Her research interest includes nondestructive testing.

CHEN MA received the B.E. degree in building electricity and intelligence from Nantong University, Nantong, China, in 2021, where she is currently pursuing the M.S. degree in control theory and control engineering. Her research interests include fault detection and diagnosis.

AIBING QIU received the Ph.D. degree in control theory and control engineering from the Nanjing University of Aeronautics and Astronautics, Nanjing, China, in 2010. He is currently a Professor with the School of Electrical Engineering, Nantong University. His research interests include fault diagnosis and fault tolerant control and their applications to smart buildings and smart grids.

LIANG HUA received the B.E. degree in electrical engineering from Nantong University, Nantong, China, in 2001, and the M.Sc. and Ph.D. degrees in control engineering from the Zhejiang University of Technology, Hangzhou, China, in 2008 and 2014, respectively. In 2001, he joined a Faculty Member of Nantong University, where he is currently a Professor and the Executive President of the School of Electrical Engineering. His research interests include power system optimization, renewable power generation, and energy storage systems.